

See discussions, stats, and author profiles for this publication at: <https://www.researchgate.net/publication/231652144>

# Phosphine-Free Synthesis of High-Quality CdSe Nanocrystals in Noncoordination Solvents: “Activating Agent” and “Nucleating Agent” Controlled Nucleation and Growth

ARTICLE *in* THE JOURNAL OF PHYSICAL CHEMISTRY C · MAY 2009

Impact Factor: 4.77 · DOI: 10.1021/jp811308h

---

CITATIONS

31

READS

21

## 2 AUTHORS, INCLUDING:



Ming Sun

Chinese Academy of Sciences

7 PUBLICATIONS 124 CITATIONS

[SEE PROFILE](#)

# Phosphine-Free Synthesis of High-Quality CdSe Nanocrystals in Noncoordination Solvents: “Activating Agent” and “Nucleating Agent” Controlled Nucleation and Growth

Ming Sun<sup>†,‡</sup> and Xiurong Yang<sup>\*,†</sup>

State Key Laboratory of Electroanalytical Chemistry, Changchun Institute of Applied Chemistry, Chinese Academy of Sciences, 5625 Renmin Street, Changchun, Jilin 130022, China, and Graduate School of the Chinese Academy of Sciences, Beijing 100039, China

Received: December 22, 2008; Revised Manuscript Received: March 25, 2009

CdSe nanocrystals (NCs) are prepared in noncoordination solvents (1-octadecene (ODE) and paraffin liquid) with long-chain primary alkylamine as the sole ligand, ODE-Se, and cadmium fatty acid salt as precursors. The obtained NCs meet the four fundamental parameters for high-quality NCs: high crystallinity, narrow size distribution, moderate photoluminescence quantum yield, and broad range size tunableness. Further, by simply regulating the relative molar ratio of alkylamine to cadmium precursor, the regular sized “nuclei” and final obtained NCs can be produced predictably within a certain size range. The size distribution of regular sized “nuclei” is very narrow ( $\text{fwhm} = 23 \pm 1 \text{ nm}$ ), and the following focusing growth procedure vanishes. This indicates a different nucleation and growth kinetics from that of the well-established “focusing” and “defocusing” theory. By analyzing the conversion factor of precursors and the concentration of magic sized nanoclusters and regular sized “nuclei”, a subtle secondary nucleation mechanism, “quantized fusion”, was proposed. First, magic sized nanoclusters are formed as the critical nuclei; second, quantized critical nuclei will couple together and fuse into perfect regular sized “nuclei” by combining with stoichiometric monomers. The “quantized fusion” transformation could be regulated by the nature and ratios of the “activating agent” and the “nucleating agent”. These transition processes are very rapid and should be kinetically controlled. The molecular mechanism for monomer formation may be based on the traditional ester aminolysis reaction.

## 1. Introduction

Colloidal semiconductor nanocrystals (SNCs) with strong “quantum confinement effects” are of great interest for both fundamental research and technical applications in optoelectronic and biomedical fields.<sup>1–4</sup> Among various semiconductor materials, group II–VI SNCs, especially CdSe NCs, have been intensively investigated due to their excellent size-dependent optical properties. CdSe is a direct gap semiconductor with bulk band gap  $\sim 1.74 \text{ eV}$  and exciton Bohr radius  $\sim 56 \text{ \AA}$ . By regulating the particle size ( $\sim 10$ – $150 \text{ \AA}$ ), the PL emission peaks of CdSe NCs could be tuned from  $\sim 450$  to  $\sim 698 \text{ nm}$ ,<sup>5–7</sup> spanning most of the visible spectrum (400–700 nm) while keeping excellent color purity ( $\text{fwhm} = 23 \pm 3 \text{ nm}$ ).<sup>8,9</sup> Besides, CdSe NCs have been providing an ideal platform to explore the nucleation and growth mechanisms of nanocrystals.<sup>10</sup> To satisfying more complicated application, various structured NCs, such as core/shell, heterostructure, and doping, have also been produced based on CdSe NCs in the past decade.<sup>11,12</sup>

In the past few years, the pyrolysis methods for CdSe NCs synthesis, which were originally reported by Bawendi’s group,<sup>5</sup> were improved greatly.<sup>11,13</sup> Green and low-cost cadmium carboxylate precursors, fatty acid ligands, and noncoordination solvents (ODE, heat transfer fluids, paraffin liquid) were used successively. Further, phosphine-free synthesis schemes were also developed based on ODE (or olive oil) solvents systems.<sup>13b,14</sup> However, CdSe NCs obtained from the phosphine-free nonco-

ordination solvent systems are generally imperfect. Besides, the size is not easily controlled, and their surface is not suitable for epitaxial growth. In this paper, a modified method is presented, and a subtle secondary nucleation mechanism is proposed.

Herein, high-quality CdSe NCs can be obtained by using a relatively lower ratio of alkylamines as the sole ligands. They can meet the four fundamental parameters: high crystallinity (sharp and multiresolved excitonic absorption peaks), narrow size distribution ( $\text{fwhm} = 25 \pm 2 \text{ nm}$ ), moderate photoluminescence quantum yield (PL QY, 5–38%), and broad range size tunableness (the first excitonic absorption peaks at 452–660 nm, PL emission peaks at 469–690 nm). By tuning the relative ratio of alkylamines to precursors, a certain sized NCs can be predictably and reproducibly synthesized, while keeping relatively high conversion of precursors. To the best of our knowledge, this may be the most effective single chemical scheme for rational control of such a broad size range of CdSe NCs.<sup>5,14,15</sup> In addition, this route possesses five potential advantages for epitaxial growth of NCs.

Further, some interesting size evolution phenomena are observed in our systems, which stimulated us to study the nucleation and growth process. Encouragingly, pure “magic” sized nanoclusters could be obtained by introducing the strong “nucleating agent” 1-dodecanethiol (DDT). Their evolution processes could be monitored facilely. By systematically and quantitatively analyzing the size and concentration of magic sized nanoclusters and regular sized “nuclei”, and the conversion factor of precursors, a microscopic and subtle secondary nucleation mechanism, “quantized fusion”, was proposed, which will significantly influence the growth kinetics. This mechanism can give some reasonable explanation for the reported size controlling phenomena of many types of NCs synthesis systems,

\* To whom correspondence should be addressed. Phone/fax: +86-431-85689278. E-mail: xryang@ciac.jl.cn.

<sup>†</sup> Changchun Institute of Applied Chemistry, Chinese Academy of Sciences.

<sup>‡</sup> Graduate School of the Chinese Academy of Sciences.

which are mainly regulated by the nature and ratio of “activating agent” and “nucleating agent”. It should be noticed that, although “magic” sized nanoclusters have been observed previously,<sup>5,7</sup> it is difficult to integrate them with the regular sized nanocrystals and study the whole nucleation and growth kinetics systematically, because those systems seem to lack something in common, such as the nature of ligands, precursors, and reaction conditions etc. Due to the presence of “activating agent”(alkylamines) as well as the absence of tri-*n*-octylphosphine (TOP) ligand, the molecular mechanism for monomer formation should be different from that of the recently reported mechanisms.<sup>16</sup>

## 2. Experimental Section

**2.1. Materials.** CdO (98.9%), stearic acid (SA, 95%), myristic acid (MA, 95%), 1-octadecylamine (ODA, 98%), *n*-dodecylamine (DA, 98+%), and 1-dodecanethiol (DDT, 96%) were purchased from Alfa Aesar. Oleic acid (OA, tech.90%), hexadecylamine (HDA, tech.90%), oleylamine (OLA, 70%), and 1-octadecene (ODE, tech.90%) were purchased from Aldrich. Tri-*n*-octylphosphine (TOP, 90%, stored in nitrogen condition) was purchased from Fluka. Coumarin 540 (98%) was purchased from Acros. Rhodamine 590 (99%) and rhodamine 610 (90%) were purchased from Sigma-Aldrich. Rhodamine 640 was purchased from Fluka. Selenium powder (Se, 99.99%), paraffin liquid (chemical grade, with boiling point higher than 300 °C), chloroform (AR), methanol (AR), and acetone (AR) were purchased from Beijing Chemical Reagent Ltd., China. Except where indicated, all chemicals and solvents were stored in ambient laboratory condition and used as received without further purification.

**2.2. Synthesis. Cadmium Precursor.** Cadmium stearate ( $\text{Cd}(\text{SA})_2$ ) and cadmium myristate ( $\text{Cd}(\text{MA})_2$ ) precursors were prepared by using the method reported previously.<sup>17</sup> Cadmium oleate ( $\text{Cd}(\text{OA})_2$ ) was prepared fresh: a mixture of 0.1 mmol of CdO, 0.4 mmol of OA, and 3 mL of ODE (or paraffin liquid) was heated at 310 °C under nitrogen for about 20 min to produce an optically clear solution.

**Selenium Precursor.** The selenium precursors (ODE-Se and TOP-Se) were prepared according to the following two methods: (a) Selenium powder (1.2 mmol) was dispersed in 20 mL of ODE at 220 °C under nitrogen for about 5 min. The obtained orange ODE-Se precursor was used fresh. (b) Selenium powder was dissolved in TOP (molar ratio = 1:1.2) via sonication for a few minutes.

**CdSe NCs.** The synthetic routes are improved based on literature methods.<sup>11,14b</sup> The reaction systems are listed in Table S1 in the Supporting Information and the consumed amount of the ligands is listed in Table S2 in the Supporting Information. For general reaction systems, 0.1 mmol of cadmium precursor ( $\text{CdM}_2$ , M = OA/SA/MA), 3 mL of ODE (or paraffin), and 1 mmol of primary alkylamine (or DDT, for synthesis magic sized nanoclusters) were mixed and degassed under dynamic vacuum for about 20 min in a reaction vessel equipped with a condenser and a thermometer. Consequently the reaction vessel was filled with nitrogen, and the temperature was raised to 285 °C. Then 0.12 mmol of selenium precursor (ODE-Se or TOP-Se) was quickly injected into the reaction vessel with vigorous stirring. The reaction temperature was then tuned down to 15 °C for the NCs growth. The reaction process was monitored by UV-vis absorption spectra. All of the first samples were collected 8–10 s after the injection.

**2.3. Characterization.** The obtained products could be dispersed in a desired solvent (toluene, chloroform, or hexane) for certain measurements. All the property measurements were performed without any postpreparative size sorting. The room

temperature PL QY was determined by comparing the PL intensity of the NCs with that of the corresponding fluorescent standard dyes.<sup>15a</sup> The TEM samples were prepared by evaporating one drop of NCs solutions on a carbon-coated copper mesh grid. The XRD samples were prepared by casting the purified NCs onto a glass wafer.

**Apparatus.** Ultraviolet-visible absorption (UV-vis abs) spectra were taken on a Cary 50 (Varian) spectrophotometer. Photoluminescence excitation (PLE) and photoluminescence (PL) spectra were recorded by a PerkinElmer-LS55 luminescence spectrometer. The observation quartz cells were both 1 cm optical path length. Transmission electron microscopy (TEM) images were collected by using a JEOL JEM-1011 transmission electron microscope operated at an acceleration voltage of 100 kV. X-ray powder diffraction (XRD) analysis was conducted on a Rigaku D/max-2500 X-ray diffractometer with graphite monochromated Cu K $\alpha$  radiation ( $\lambda = 1.5418 \text{ \AA}$ ).

**Conversion Factor Calculation.** The samples were prepared by a series of individual experiments under the same conditions. The NCs growth was quenched by toluene. Then, the original products were diluted to the same volume for the optical density measurement. The conversion factor of precursors was calculated by combining the NCs size, concentration, crystalline lattice structure (zinc blende or wurtzite), and crystalline cell parameter of bulk crystal (CdSe, zinc blende,  $a = 6.05 \text{ \AA}$ ; wurtzite,  $a = 4.29 \text{ \AA}$ ,  $c = 7.01 \text{ \AA}$ )<sup>18,19</sup> together. The diameter and concentration of the NCs at a given moment were calculated by the reported procedure.<sup>8</sup> For the magic sized nanoclusters, the molar extinction coefficient was roughly estimated according to the literature.<sup>7a,c</sup>

## 3. Results and Discussions

**3.1. Reaction System.** Solvents were selected based on the low-toxicity and low-cost principle. ODE was an ideal solvent system for studying the nucleation and growth kinetics, because of its purity and moderate viscosity. Paraffin liquid, which is composed of long-chain alkanes ( $\text{C}_{16}\text{--C}_{20}$ ), was chosen as a model solvent system to represent those complicated noncoordination solvents, such as heat transfer fluids etc. The growth trend in paraffin liquid is illustrated in Figure S1 (Supporting Information), with PL QY ~29% and fwhm ~25 nm. The combination of precursor and ligand is important for the noncoordination solvent system. Compared to  $\text{Cd}(\text{SA})_2$  and  $\text{Cd}(\text{MA})_2$ ,  $\text{Cd}(\text{OA})_2$  is a relatively stable precursor that could be coheated with a higher ratio of alkylamines (DDA, HDA, or ODA) at high temperature (280–320 °C). Accordingly,  $\text{Cd}(\text{OA})_2$  and HDA were selected as the research system. Correspondingly, injection and growth temperature are executed at a moderate reaction temperature (265–285 °C). Combining the recent research results,<sup>15b</sup> the reaction temperature can be further lowered if alkylamines with a lower boiling point were used.

**3.2. Optical Properties.** For CdSe NCs obtained from system 1, the time evolution absorption, PL, and PLE spectra are shown in Figures 1 and 2. Four different ratios of alkylamines are used (see Table S1 in the Supporting Information). The absorption and PLE spectra possess sharp and multiresolved electronic transitions. For larger NCs, the features of the excitonic absorption peaks can increase to 7 (Figure 1e (inset in panel c), QY ≈ 20%). For the high-quality samples ( $\text{abs} \approx 458\text{--}620 \text{ nm}$ ), the value of full width at half-maximum (fwhm) of the PL spectra is  $24 \pm 2 \text{ nm}$  (Figure S2, Supporting Information). The parameters mentioned above indicate very narrow size distribution and high

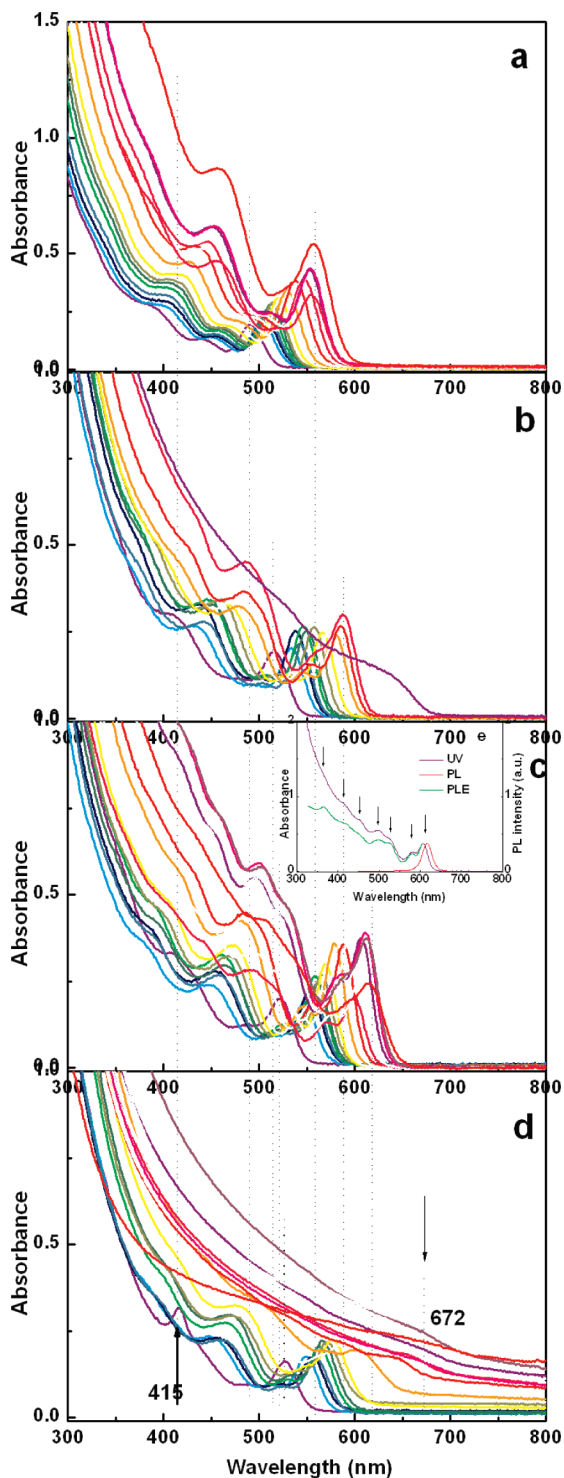


**Figure 1.** UV-vis absorption spectra (a–e) and PLE spectra (e) of as-prepared CdSe NCs from system 1 with different amounts of HDA: (a) 1, (b) 2, (c) 3, and (d) 4 mmol.

crystallinity of the obtained NCs, and are comparable with the best CdSe samples reported previously.<sup>5,8,9,14c,15a,20</sup> The small value of the Stokes shift (from 14 to 9 nm with increased size) indicates low aspect ratio for wurtzite structured CdSe NCs<sup>5,21</sup> and band-edge dominated luminescence. From the growth process monitored by UV-vis abs and PLE spectra, we can see that the energy gap between the first ( $1S_{3/2}1S_e$ ) and second ( $2S_{3/2}1S_e$ ) exciton transition peaks decreases gradually as the particles grow in size, indicating the structure transformation from ZB to WZ.

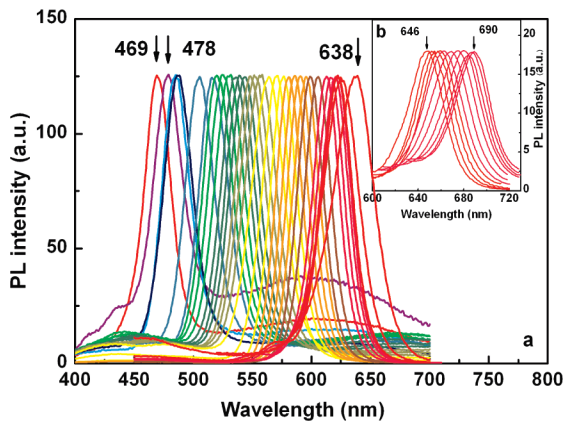


**Figure 2.** PL spectra of as-prepared CdSe NCs from system 1 with different amounts of HDA.

phase.<sup>14b,c</sup> The differences in the absorption spectra originate from the different electronic energy band structure of the two-crystal phase, which will induce a different crystal field and Brillouin zone.<sup>22</sup>

The PL QY is significantly influenced by the NCs' surface state, such as the stoichiometric atom ratio of Se:Cd, the nature and coverage ratio of the capping agent, and the polarity of the dispersing solvent.<sup>15a,23</sup> For system 1, a lower molar ratio of Se/Cd precursors (~1.2) and a lower ratio of alkylamines ligands are used, which will restrain the improvement of PL QY. Alkylamines are considered as effective Lewis bases (electron donors), which will bind to surface Cd sites on CdSe NCs.<sup>23a</sup> By increasing the relative ratio of alkylamines, the PL QY value will be improved (Figure S2, Supporting Information). However, the selenium surface sites remain naked,<sup>14b,23a</sup> which will produce a large number of dangling bonds to act as traps for the photogenerated charge, and lower the intracrystal recombination of electron and hole. In summary, the PL QY is 5–38% in the wavelength window from 490 to 650 nm, while lower than 5% below 490 nm and above 650 nm (Figure S2, Supporting Information).

**3.3. TEM and XRD Analysis.** The size, shape, and crystal structure were further studied by the TEM and XRD. Large-area monodisperse NCs could be observed from the TEM images (Figure 3, Figure S3 in the Supporting Information). The dot shaped NCs can form well-ordered two-dimensional superlattice and one-dimensional nanostructure with a pearl necklace pattern, which demonstrate that the size and shape of the particles are uniform. The driving force for one-dimensional coupling may be the dipole moment.<sup>24</sup> Inspired by these phenomena, a facile route based on oriented attachment mechanisms<sup>25</sup> could be designed to synthesize nanorods or nanowire that will eliminate the use of expensive alkylphosphonic acids.<sup>11</sup> The morphology of NCs changed gradually from cubic to hexagonal with increased diameter, indicating structural transition from zinc blende to wurtzite, which was further proved by the corresponding XRD patterns (Figure 4). By comparing the absorption and PLE spectra, we can find that the ligand composition will influence phase transition strongly (Figure 1, as well as Figures S4 and S5 in the Supporting Information). When pure fatty acid ligands are used, the zinc blende crystal structure can exist stably at high temperature (Figure S5, Supporting Information). When alkylamine (or alkylamines/TOP) ligands are used, the phase transition phenomena will emerge as the NCs size increases (Figure 1, as well as Figure S4 in the Supporting Information).

**3.4. Nucleation and Growth Kinetics.** By observing Figure 1, there are three interesting and related phenomena that promote

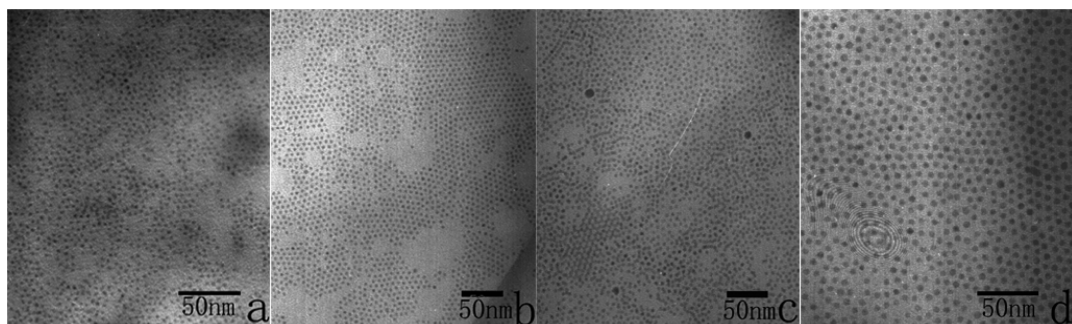


**Figure 3.** TEM images of four samples obtained from system 1: (a) 2.5, (b) 3.6, (c) 4.5, and (d), 5.5 nm.

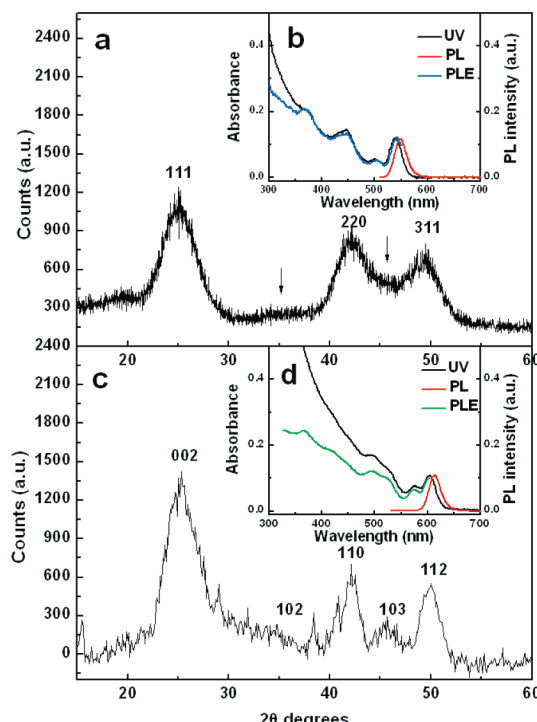


**Figure 4.** XRD of two samples obtained from system 1 with different crystalline lattice structures: (a) zinc blende and (b) wurtzite.

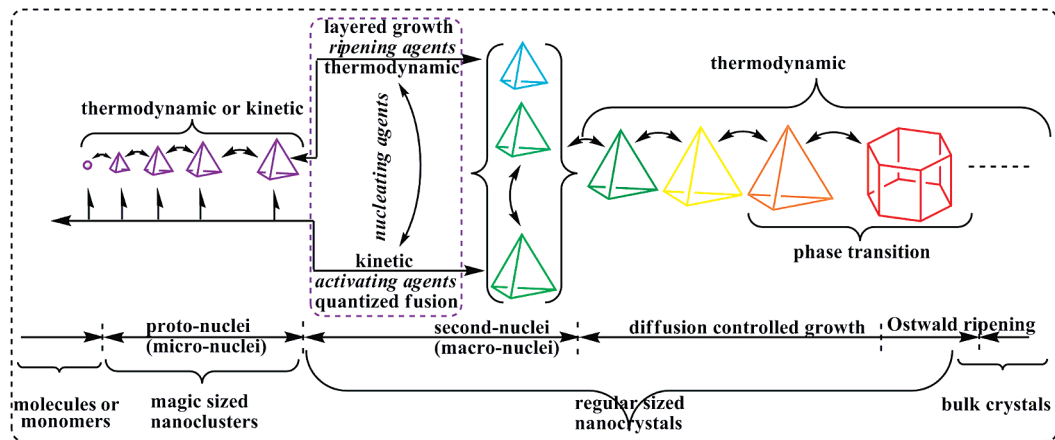
us to study the nucleation and growth process: (1) The size distribution of the initial regular sized “nuclei” is very narrow ( $\text{fwhm} = 23 \pm 1 \text{ nm}$ , Figure 1), and will remain nearly constant ( $\text{fwhm} = 25 \pm 2 \text{ nm}$ ) during the whole growth period, which is not consistent with the traditional “focusing” and “defocusing” processes.<sup>10</sup> (2) The diameter of the initial regular sized “nuclei” and the final obtained NCs will increase by increasing the ratio of alkylamines. This phenomenon is reverse to the reported experimental result.<sup>10d,20</sup> (3) The growth of NCs will terminate at a certain size and the size distribution will remain narrow for a relatively long time before Ostwald ripening. These unusual phenomena may be induced by the unique ligand composition of system 1, which only contains alkylamines. To further identify the ligands effect, another five systems are introduced (systems 2–6, Table S1, Supporting Information) to study the nucleation and growth kinetics.

For convenient discussion, the regular sized NCs, which were obtained  $\sim 8\text{--}10 \text{ s}$  after the injection, are defined as “macroscopic nuclei” (“macro-nuclei”). Correspondingly, “microscopic nuclei” (“micro-nuclei”) are defined for the magic sized nanoclusters, which appeared far before “macro-nuclei” and can be observed at the high-energy side of the absorption spectra but are not easy to distinguish by TEM (Scheme 1).<sup>11</sup>

**3.4.1. First: Growth Process Analysis.** The size fixing phenomena have been observed in various NCs synthesis systems, including semiconductor, metal oxide, and noble metal (Table S4, Supporting Information). By using the final size as a probe, Weller et al. deduced inversely that the size was controlled by balancing the rate of nucleation and growth,<sup>26</sup> which may be general for the above-mentioned systems. However, this mechanism seems lacking of systemic and quantitative analysis, because the nucleation and growth processes of CoPt<sub>3</sub> NCs are difficult to control and monitor. For CdSe NCs (even cluster molecule), the strong size-dependent optoelectronic properties will serve as an excellent spectroscopic probe to provide microscopic experimental details of nucleation.

In system 1–2, although the NCs can be fixed at a certain size, Ostwald ripening will emerge after a long heating time. This indicates that the conversion factor of precursors is very high and the monomer concentration is very low at the final growth stage.<sup>10,27</sup> Reasonably, the consumed monomers can be considered equivalent for each condition of system 1–2 (Figure 1, Figure S4 in the Supporting Information). So, the final size should be regulated by the initial concentration of “macro-nuclei” and the residual monomers after nucleation. To confirm this hypothesis, the concentration of NCs and the conversion factor of the cadmium precursors are calculated quantitatively (Cd/Se atom ratio of CdSe NCs  $\sim 1\text{--}1.2$ )<sup>23a</sup> (systems 1, 2, 4, and 5, Table 1–3), which can be used to systematically analyze the nucleation and growth kinetics. The amount of alkylamine, the time point, the parameter for comparison, and the quantitative calculation result are listed in detail at Tables 1–3. The corresponding absorption spectra are shown in Figure 5. The calculation methods are described in the Experimental Section. Although all of the samples are prepared from individual experiment, the ensemble size and concentration evolution tendencies are reliable, because these results are obtained from ample and reproducible experiments.

For system 1, three groups of samples are prepared with different ratios of alkylamines. The representative time points are selected according to the growth curve of Figure 1. Via integrated intersystem comparison (Figure 5a, Table 1), we can find that the concentration decreases with the increasing ratio of HDA. This result seems to agree with the reported conclusion:<sup>10d,26</sup> the nuclei number will decrease as the ratio of ligands (containing carboxylic acid groups) increases, and a larger final particle will be produced. However, some subtle differences coexist at the nucleation stage: (1) the size of the initial “macro-nuclei” will become larger as the alkylamine concentration increases and (2) the conversion factors of cadmium precursors are larger than the theoretical calculation (2–8%),<sup>10d</sup> and they will not decrease obviously at an early age (<15 s) when the amount of alkylamine increases. Accord-

**SCHEME 1:** Schematic Illustration of the Possible Evolution Pathways for the Magic Sized Nanoclusters and the Whole Nucleation and Growth Processes of the Nanocrystals**TABLE 1:** Samples Obtained from System 1 with Different Amounts of HDA (mmol)<sup>a</sup>

1 mmol HDA	8 s	15 s	300 s
first absorption peak (hwhm)	472 nm (15 nm)	503 nm (16 nm)	528 nm (16 nm)
NCs concn	$5.23 \times 10^{-5}$ mol/L	$6.37 \times 10^{-5}$ mol/L	$5.72 \times 10^{-5}$ mol/L
conversion factor	23.3%	40.3%	50.5%
2 mmol of HDA	8 s	15 s	1200 s
first absorption peak (hwhm)	503 nm (14 nm)	533 nm (15 nm)	554 nm (16 nm)
NCs concn	$4.17 \times 10^{-5}$ mol/L	$3.64 \times 10^{-5}$ mol/L	$3.26 \times 10^{-5}$ mol/L
conversion factor	26.3%	35.3%	46.5%
3 mmol of HDA	8 s	15 s	1800 s
first absorption peak (hwhm)	505 nm (15 nm)	548 nm (15 nm)	588 nm (15 nm)
NCs concn	$2.64 \times 10^{-5}$ mol/L	$2.60 \times 10^{-5}$ mol/L	$2.24 \times 10^{-5}$ mol/L
conversion factor	16.9%	32.9%	71.4%

<sup>a</sup> There are three key parameters: CdSe NCs concentration (mol/L) vs. time (s, second); conversion factor of cadmium precursors (%) vs. time; and the first excitonic absorption peak and hwhm (nm) vs. time. The corresponding absorption spectra are shown in Figure 5a.

ingly, some different nucleation mechanisms are considered to exist in system 1, which may be induced by the nature of the ligands.

**3.4.2. Second: Subtle Nuclei Evolution Mechanism Consideration.** By changing the reaction conditions, such as temperature, viscosity of solvent, and ligands composition etc. (systems 1–5), a series of discrete feature absorption peaks can be observed at the high-energy side of the absorption spectra (Figures 1 and 5–7, as well as Figures S1, S4, and S6 in the Supporting Information). They are considered as magic sized nanoclusters with defined molecular structure and close-shell configuration.<sup>7,11</sup> Their size is about 0.7–2 nm,<sup>7a,e</sup> consistent with the calculated diameter of “critical-nuclei” (0.6–1.1 nm).<sup>10d</sup> They are summarized and compared with the literature results in Table S3 in the Supporting Information.

For system 1, the absorption peak at ~415 nm can be observed obviously when relatively higher ratios of alkylamines are used (Figure 1d). There are no intermediate absorption peaks between magic sized nanoclusters and regular sized NCs (“macro-nuclei”), and the size gap is proportional to the amount of alkylamine. However, when OA is used as the sole ligand (system 6), the size of the “macro-nuclei” is not as sensitive to the ratio of the ligand (Figure S5, Supporting Information). The size gap, which lies between the smallest “macro-nuclei” (abs ~435 nm, Figure S5, Supporting Information) and the larger

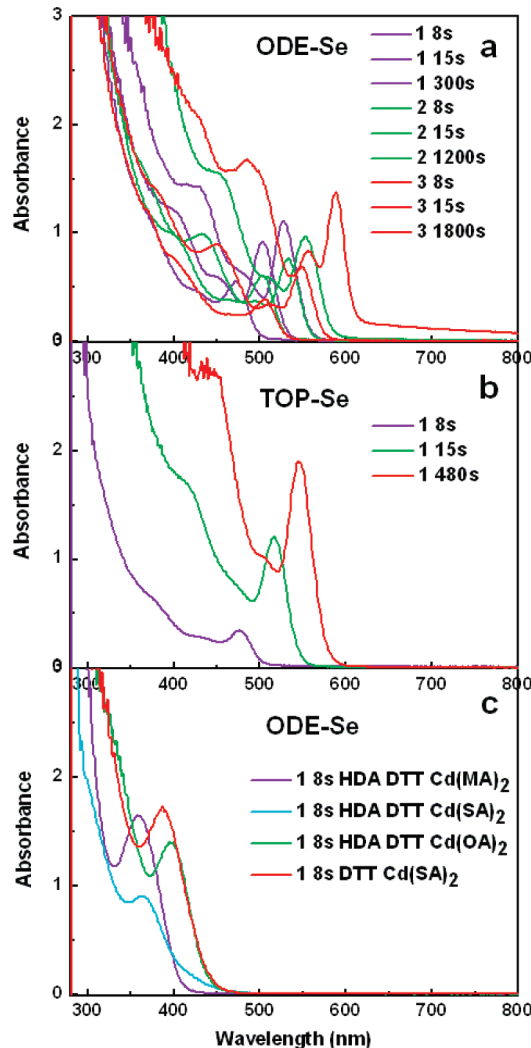


**Figure 5.** (a) System 1: Absorption spectra of CdSe NCs at different reaction times with different amounts of HDA (purple, 1 mmol; green, 2 mmol; red, 3 mmol; Table 1). (b) System 2: Absorption spectra of CdSe NCs at different reaction time with 1 mmol of HDA (Table 2). (c) System 4–5: Absorption spectra of CdSe NCs at the same reaction time with DDT ligand (Table 3).

magic sized nanoclusters (abs ~431 nm),<sup>7c</sup> is very small. Besides, the final particles sizes are similar (Figure S5g, Supporting Information), which indicates that the initial concentration of “macro-nuclei” is not easily tuned. When TOP is introduced

**TABLE 2: Samples Prepared in System 2<sup>a</sup>**

1 mmol HDA + 0.25 mmol TOP	8 s	15 s	480 s
first absorption peak (whhm)	476 nm (15 nm)	517 nm (15 nm)	546 nm (16 nm)
NCs concn	$3.11 \times 10^{-5}$ mol/L	$7.04 \times 10^{-5}$ mol/L	$1.46 \times 10^{-4}$ mol/L
conversion factor	14.4%	53.6%	89.8%

<sup>a</sup> TOP ligands are introduced. The corresponding absorption spectra are shown in Figure 5b.

(system 2), another interesting phenomenon can be observed. Although uniform “macro-nuclei” (fwhm = 25 ± 1 nm) can be formed after injection (<8 s), the ensemble size distribution will become broad from ~20 to ~150 s (fwhm = 32–47 nm), then narrow again at the following growth stage (fwhm = 29 ± 3 nm). During the broadening stage, two continued and adjacent absorption peaks and asymmetric emission spectra can be observed (Figures S4 and S7, Supporting Information), indicating the coexistence of two different sized NCs. The smaller NCs should be the newly formed “macro-nuclei”. Indeed, the concentration of NCs increased after this stage (Table 2). Compared to system 1, the conversion rate of precursors is also increased (Table 2). This indicates that the nucleation process is partly hindered and delayed.

How can the above-mentioned differences among systems 1, 2, and 6 be interpreted? Obviously, these differences are induced by the nature of the ligands, which influences the evolution mode of magic sized nanoclusters (“micro-nuclei”) significantly.

In system 6, OA can be considered as a “ripening agent”, which will disturb the formation of critical nuclei.<sup>19</sup> The absorption peaks of the initial “macro-nuclei” are unsharp and indistinct, indicating that they are nonuniform and imperfect (Figure S5, Supporting Information). The imperfect smaller regular sized CdSe NCs could be gradually etched into perfect magic sized nanoclusters by accurate amine titration.<sup>7d</sup> This result reversely demonstrates a thermodynamic controlled “layered growth” mode for magic sized nanoclusters. The “layered growth” can be realized refinedly by regulating the composition of the ligands (system 3), which will be discussed in the following paragraph. Accordingly, the “layered growth” mode seems suitable for system 6 (Scheme 1).

In system 1, the growth mode should be different, because an “activating agent” (alkylamine) is used as the sole ligand. Alkylamines will promote the decomposition of metal fatty acid salt to form supersaturated monomers, and then burst forth numerous thermodynamic metastable magic sized nuclei (“micro-nuclei”). Because of the absence of a “ripening agent”, the lattice atoms will not be detached from nascent nuclei easily. A large amount of magic sized nuclei will be left with a natural crystal structure and a narrow size distribution. Their concentration may reach the supersaturation level, which will induce the secondary nucleation.<sup>27</sup> By introducing DDT (a strong “nucleating agent”<sup>11,19</sup>) into system 1 (systems 4 and 5), pure magic sized nanoclusters can be obtained. According to the absorption spectra obtained at ~8 s (Figure 5c), their concentration can be roughly calculated (Table 3), which are 10-fold more than that of “macro-nuclei” (Table 1). For smaller nanoclusters, with an absorption peak at ~280 nm<sup>28b</sup> or ~296 nm,<sup>7a</sup> the concentration may be higher. Obviously, the residual monomers (Table 3) are not enough to support all of these magic sized nanoclusters growing into “macro-nuclei” by the “layered growth” mode. Again, it seems that there is a secondary nucleation process for magic sized nanoclusters.

Now, another two correlated evolution mechanisms for clusters should be introduced: (1) “quantized aggregation”,<sup>28a–c,30</sup> which speculates that quantized numbers of nanoclusters can aggregate together with fractal geometry,<sup>28</sup> and (2) “cluster fusion”,<sup>29</sup> where certain numbers of magic sized nanoclusters can fuse into uniform larger nanoclusters by combining stoichiometric monomers. The crystal structure for the larger one is analogous to the original nanoclusters or the bulk lattice. This process is conjectured to be the rapid exchange of metal, chalcogenide, and ligands inter(and intra)-clusters.<sup>31</sup> The aggregation and fusion processes should be kinetic controlled,<sup>25</sup> because the critical points are sensitive to the synthesis parameters,<sup>28–30</sup> such as the size and concentration of the critical nuclei, the nature of surface ligands, the amount of monomers, etc. Accordingly, secondary nucleation may be attributed to the combination of “quantized aggregation” and “cluster fusion”. This combination will be abbreviated to “quantized fusion” in the following paragraph (Scheme 1). The “quantized fusion” is similar to the kinetic controlled biomineralization (or oriented attachment) processes.<sup>25</sup> It will provide a relatively lower energy barrier for magic sized nanoclusters to overcome and grow into perfect regular sized NCs. This process should be very rapid, if it is not instantaneous, because no intermediate sized clusters/crystals between them can be observed.

Further, we will analyze the potential driving force and disturbing factors for “quantized fusion” in system 1. As discussed above, there are two stages for “quantized fusion”: “quantized aggregation” and “fusion” (or atomic rearrangement). On the basis of the oriented attachment mechanism,<sup>24,25</sup> the dipole moments should be the major driving force for “quantized aggregation”. For the magic sized nanoclusters of CdSe, the crystal structure is conjectured to be cage-like or zinc blende.<sup>7</sup> However, for such small clusters, the structure may be imperfect, which will induce asymmetric shape. Besides, large numbers of dangling bonds should exist on the surface, especially for the naked Se atoms, which increase the surface localized charge and dielectric constant. Both of them will increase the intrinsic permanent dipole moments.<sup>24b</sup> High reaction temperature and high concentration will increase the collision frequency, and combined with the low facet selectivity of alkylamines,<sup>32</sup> the aggregation probability can also be increased. In the following “fusion” process, “nucleating agents” may be the key disturbing factor. Strong “nucleating agents” will bind strongly to the particle surface and form insoluble surface precipitates, kinetically hindering both the dissolution and growth of fresh nuclei.<sup>19</sup> Alkylamines can be considered as a weak “nucleating agent”, because they coordinate to the NCs surface with dynamic equilibrium under appropriate temperature.<sup>15b</sup> They will not disturb the “fusion” intensively. Accordingly, the “quantized fusion” could be realized relatively easily in system 1.

When a moderate “nucleating agent” TOP is introduced (system 2), the aggregation and “fusion” will be partly hindered because TOP will coordinate to the surface selenium atoms and be difficult to remove completely.<sup>19,33</sup> The disturbance can be reflected by the above-mentioned special nucleation process of system 2. In this condition, a higher concentration of smaller “macro-nuclei” is formed, which will induce the size of the final obtained NCs to decrease. Recently, a similar experimental phenomenon was reported, in which smaller CdSe NCs will be obtained by increasing the ratio of TOP to oleylamine.<sup>34</sup> However, the influence of TOP can be lowered when the ratio of “activating agent” (HDA) increases. This can be reflected by the increased symmetry of the PL spectra at the initial growth stage (Figures S4e and S7, Supporting Information).

**TABLE 3: Samples Prepared in Systems 4 and 5<sup>a</sup>**

system 4: 1 mmol HDA + 0.8 mmol DDT	Cd(MA) <sub>2</sub>	Cd(SA) <sub>2</sub>	Cd(OA) <sub>2</sub>	system 5: 0.8 mmol DDT Cd(SA) <sub>2</sub>
absorption peak (hwhm)	358 nm (24 nm)	364 nm (25 nm)	396 nm (23 nm)	387 nm (28 nm)
NCs concn	$\sim 5.61 \times 10^{-4}$ mol/L	$\sim 4.92 \times 10^{-4}$ mol/L	$> 5.12 \times 10^{-4}$ mol/L	$> 6.24 \times 10^{-4}$ mol/L
conversion factor	~46.4%	~40.5%	~79.7%	~97.1%

<sup>a</sup> DDT ligands are introduced. All of the samples are collected at 8 s after injection Se precursors. The corresponding absorption spectra are shown in Figure 5c.

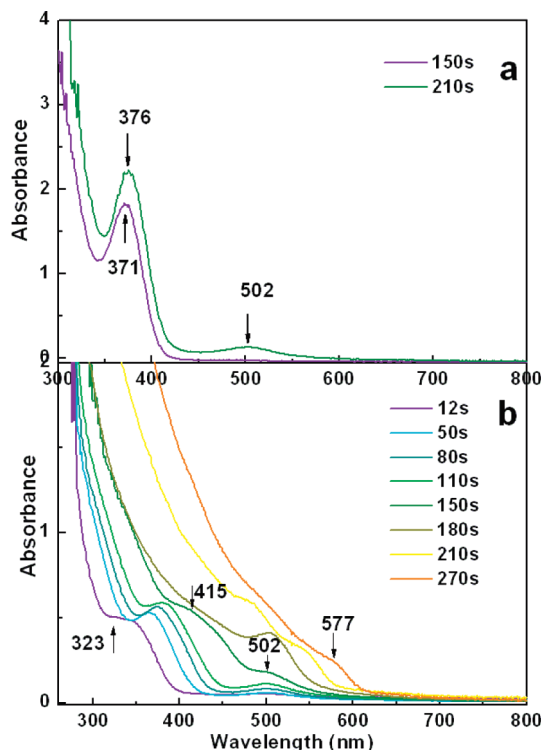


**Figure 6.** UV-vis absorption spectra of as-prepared CdSe NCs at the different reaction times of system 3: (a) HDA and DDT as ligands and (b) DDA and DDT as ligands.

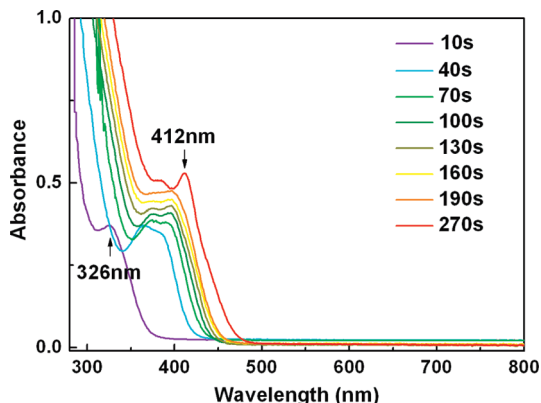


**Figure 7.** UV-vis absorption spectra of as-prepared CdSe NCs at the different reaction times with ODA and DDT as ligands in system 3.

When a strong “nucleating agent” DDT is introduced (system 3), the aggregation and “fusion” will be strongly inhibited. The evolution process of magic sized clusters can be slowed and monitored by absorption spectra. In only in few cases can the size transition be observed between smaller clusters (abs < 412 nm) and regular sized NCs (abs ~ 502 nm) (Figure 6). In most cases, the absorption peak cannot exceed ~412 nm (Figure 7), which corresponds to a low-temperature stable magic sized nanoclusters ( $d \approx 1.2\text{--}1.7$  nm).<sup>5,7,28b</sup> Further, by carefully

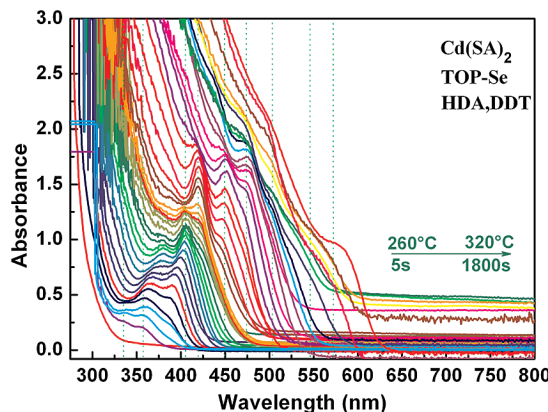


**Figure 8.** UV-vis absorption spectra of as-prepared CdSe NCs at the different reaction times of system 3. In this method, Cd(SA)<sub>2</sub> and TOP-Se are used as precursors, while HDA and DDT are used as ligands. The reaction temperature increases from 260 to 320 °C during the growth process.

regulating the reaction parameters, such as ligands, precursors, temperature, etc., a refined “layered growth” process can be realized (Figure 8). The continuous red shift of the absorption peak (~330–475 nm) indicates a consecutive growth of the magic sized nanoclusters. The evolution of the size can sequentially span across the whole family of magic sized nanoclusters (abs > 330 nm, Table S3, Supporting Information), and extend to the regular sized region. Compared to the recently reported sequential growth phenomena,<sup>7c</sup> the transformation of the absorption spectra of system 3 is more smooth, indicating the accurate attachment of atoms. Obviously, this growth mode is distinct from that of the above-mentioned “quantized fusion” mechanism.

The volume conservation should also be considered for “quantized fusion”, which can be calculated from some special transition point. According to the size evolution process of Figure 6, the obtained regular sized NCs (NCs<sub>502</sub>, abs ~502 nm, diameter ~2.364 nm<sup>8a</sup>) can be tentatively hypothesized as the transition result of a smaller cluster molecule (Cd<sub>8</sub>Se<sub>13</sub>, abs ~296 nm, equivalent spherical diameter ~0.7 nm<sup>7a,e</sup>). NCs<sub>502</sub> is 38.52 times the volume of Cd<sub>8</sub>Se<sub>13</sub> clusters. The decimal fraction may represent the additional stoichiometric monomers during the aggregation and fusion processes. This value will decrease if the aggregation is built by the smallest clusters. It is noteworthy that the (CdSe)<sub>3</sub> cluster is proposed as the smallest nucleus based on the combination of ab initio DFT calculations and experimental spectra.<sup>7g</sup> However, its volume is difficult to determine.

Two other recently reported larger families of CdSe magic sized NCs should also be noted: NCs<sub>463</sub> (abs ~463 nm, diameter ~2.05 nm<sup>8a</sup>) and NCs<sub>513</sub> (abs ~513 nm, diameter ~2.48 nm<sup>8a</sup>) can be synthesized in pure form under special conditions.<sup>7f</sup> NCs<sub>463</sub> (NCs<sub>513</sub>) is 25.12 (44.47) times the volume of Cd<sub>8</sub>Se<sub>13</sub> clusters. In systems 1 and 2, for the “macro-nuclei” obtained at 8 s, the first excitonic absorption peaks are well above (or overlap) 463 or 513 nm as the amounts of HDA increase (Figure

1, as well as Figure S4 and Table S2 in the Supporting Information). In contrast, in system 6, lacking an “activating agent” (HDA), the first excitonic absorption peaks are ambiguous and do not easily exceed 463 nm (Figure S5 and Table S2 in the Supporting Information). These results indicate that NCs<sub>463</sub> (or NCs<sub>513</sub>) can act as the critical point for secondary nucleation, and become the beginning point for the growth of regular sized NCs. Their concentration will remain constant until Ostwald ripening emerges. The unconverted nanoclusters will decompose into monomers to support the growth of regular sized NCs, which is consistent with the reported heterogeneous growth mechanism.<sup>30d</sup>

Integrating the above-mentioned discussion, the secondary nucleation, which is induced by “quantized fusion”, can explain the discontinuous (or discrete) size evolution phenomena of system 1. Encouragingly, the proposed “quantized fusion” mechanism can also provide a reasonable explanation for some reported size controlling phenomena of many types of NCs synthesis systems (summarized in Table S4, Supporting Information). In those systems, the size is mainly regulated by the ratios of “activating agent” and “nucleating agent”. For comparison, some typical “ripening agent” (or “nucleating agent”) dominated size controlling systems are also listed in Table S4 (Supporting Information). It is noteworthy that the exact function of a certain agent is determined by the whole nature of the reaction system.

**3.4.3. Third: Possible Molecular Mechanism for Monomer Formation.** For system 1, ODE-Se is used as a precursor instead of TOP-Se, which makes the P=Se bond cleavage procedure nonexistent.<sup>16</sup> Accordingly, the well-known ester aminolysis reaction, which involves the nucleophilic attack of an amine group on the carbonyl carbon atom of metal carboxylate,<sup>35</sup> should be considered beforehand. The detailed molecular mechanism needs further intensive experimental investigation.

**3.5. Advantage for Epitaxial Growth.** Epitaxial growth of various inorganic shells and conjugation of robust organic protection layers are needed to improve the PL QY and stability.<sup>36,37</sup> By considering the surface geometry, surface energy, facet selectivity, and binding energy of ligands,<sup>32</sup> three advantages for epitaxial growth could be predicted for the CdSe core prepared in system 1. First, the selenium surface sites are naked, which will make the cation more easily couple with the selenium atoms.<sup>37b</sup> Second, unlike alkylphosphine species,<sup>33</sup> alkylamines bond reversibly to the NCs surface, which will decrease the barrier between anion and cadmium atoms.<sup>37b</sup> Further, because the surface bonding dynamics equilibrium is related to the boiling point of alkylamines and temperature,<sup>15b</sup> suitable alkylamines and corresponding cation (or anion) precursors could be selected for epitaxial growth at moderate temperature. Third, the uniform shape and narrow size distribution will provide similar surface chemical potential and diffusion coefficient for homogeneous growth of the ensemble shell layers, and the Ostwald ripening will be postponed.<sup>10,27</sup> Inspired by the aforementioned growth process, two other advantages for in situ epitaxial growth emerge naturally: (1) certain sized core NCs could be obtained leisurely and (2) conversion factors of the precursors are very high, which will simplify the purification step and keep the NCs surface perfect. Besides, the “quantized fusion” mechanism may provide a new aspect to designing the synthesis routes for doped and alloyed NCs.

## 4. Conclusions

Significant improvements have been made for the synthesis of high-quality CdSe NCs in phosphine-free noncoordination

solvents by using a smaller amount of alkylamine as the sole multifunctional ligand. A certain sized NCs can be predictively and reproducibly synthesized across a broad size range, with relatively high conversion factor of the precursors. The synthetic route possesses five potential advantages for epitaxial growth. Additionally, a new route for synthesis magic sized nanoclusters is also contributed. Further, a “quantized fusion” controlled secondary nucleation mechanism is conjectured. The “quantized fusion” transition can be regulated by the nature and ratio of the “activating agent” and the “nucleating agent”, and will significantly influence the following growth kinetics. This mechanism can give a reasonable explanation for the size controlling phenomena of many types of NCs, and will inspire us to optimize the synthetic routes rationally. However, the intrinsic transformation mechanisms still need further intensive experimental and theoretical investigation. If the systems could be monitored by in situ techniques (such as in situ UV-visible spectroscopy, synchrotron SAXS/WAXS, etc.),<sup>10c,38</sup> more microscopic nucleation and growth processes will be observed and the quantitative analysis will be more accurate, and the initial structure of nanoclusters may be identified simultaneously. For the future, to eliminate environmental pollution completely, high-quality and low-toxicity optoelectronic materials (such as doped SNCs, rare-earth NCs, etc.<sup>39</sup>) should be explored to promote the Green-Tech revolution.

**Acknowledgment.** This work was supported by the National Natural Science Foundation of China (No. 90713022), the National Key Basic Research Development Project of China (No. 2007CB714500), and the Project of Chinese Academy of Sciences (No. KJCX2.YW.H09), (No. KJCX2.YW.H11). The authors acknowledge Mr. Li Qi, Guangtao Song, Haizhou Yu, and Xianfeng Hao for their valuable discussions on the nucleation and growth kinetics.

**Supporting Information Available:** Synthesis systems of this paper; summarized families of magic sized nanoclusters; “activating agent”, “ripening agent”, or “nucleating agent” dominated size controlling systems; higher magnification TEM images, UV-vis absorption spectra, PL spectra, PL quantum yields, mean particle size, and fwhm of as-prepared CdSe NCs in different conditions and systems. This material is available free of charge via the Internet at <http://pubs.acs.org>.

## References and Notes

- (1) Alivisatos, A. P. *Science* **1996**, *271*, 933–937.
- (2) Coe, S.; Woo, W. K.; Bawendi, M. G.; Bulovic, V. *Nature (London)* **2002**, *420*, 800–803.
- (3) Klimov, V. I. *J. Phys. Chem. B* **2006**, *110*, 16827–16845.
- (4) Michalet, X.; Pinaud, F. F.; Bentolila, L. A.; Tsay, J. M.; Doose, S.; Li, J. J.; Sundaresan, G.; Wu, A. M.; Gambhir, S. S.; Weiss, S. *Science* **2005**, *307*, 538–544.
- (5) (a) Murray, C. B.; Norris, D. J.; Bawendi, M. G. *J. Am. Chem. Soc.* **1993**, *115*, 8706–8715. (b) Murray, C. B.; Kagan, C. R.; Bawendi, M. G. *Annu. Rev. Mater. Sci.* **2000**, *30*, 545–610.
- (6) Wang, Q. B.; Seo, D.-K. *Chem. Mater.* **2006**, *18*, 5764–5767.
- (7) (a) Soloviev, V. N.; Eichhofer, A.; Fenske, D.; Banin, U. *J. Am. Chem. Soc.* **2000**, *122*, 2673–2674. (b) Kasuya, A.; Sivamohan, R.; Barnakov, Y. A.; Dmitruk, I. M.; Nirasawa, T.; Romanyuk, V. R.; Kumar, V.; Mamkin, S. V.; Tohji, K.; Jeyadevan, B.; Shinoda, K.; Kudo, T.; Terasaki, O.; Liu, Z.; Beloludov, R. V.; Sundararajan, V.; Kawazoe, Y. *Nat. Mater.* **2004**, *3*, 99–102. (c) Kudera, S.; Zanella, M.; Giannini, C.; Rizzo, A.; Li, Y. Q.; Gigli, G.; Cingolani, R.; Ciccarella, G.; Spahl, W.; Parak, W. J.; Manna, L. *Adv. Mater.* **2007**, *19*, 548–552. (d) Landes, C.; Braun, M.; Burda, C.; El-Sayed, M. A. *Nano Lett.* **2001**, *667–670*. (e) Soloviev, V. N.; Eichhofer, A.; Fenske, D.; Banin, U. *J. Am. Chem. Soc.* **2001**, *123*, 2354–2364. (f) Ouyang, J.; Zaman, B.; Yan, F.; Johnston, D.; Li, G.; Wu, X.; Leek, D.; Ratcliffe, C. I.; Ripmeester, J. A.; Yu, K. *J. Phys.*

- Chem. C* **2008**, *112*, 13805–13811. (g) Jose, R.; Zhanpeisov, N. U.; Fukumura, H.; Baba, Y.; Ishikawa, M. *J. Am. Chem. Soc.* **2006**, *128*, 629–636.
- (8) (a) Yu, W.; Qu, L.; Guo, W.; Peng, X. *Chem. Mater.* **2003**, *15*, 2854–2860. (b) Talapin, D. V.; Nelson, J. H.; Shevchenko, E. V.; Aloni, S.; Sadtler, B.; Alivisatos, A. P. *Nano Lett.* **2007**, *7*, 2951–2959.
- (9) Wu, D. G.; Kordesch, M. E.; Van Patten, P. G. *Chem. Mater.* **2005**, *17*, 6436–6441.
- (10) (a) Talapin, D. V.; Rogach, A. L.; Haase, M.; Weller, H. *J. Phys. Chem. B* **2001**, *105*, 12278–12285. (b) Peng, X. G.; Wickham, J.; Alivisatos, A. P. *J. Am. Chem. Soc.* **1998**, *120*, 5343–5344. (c) Qu, L. H.; Yu, W. W.; Peng, X. *Nano Lett.* **2004**, *4*, 465–469. (d) Bullen, C. R.; Mulvaney, P. *Nano Lett.* **2004**, *4*, 2303–2307.
- (11) Peng, X. G.; Thessing, J. *Struct. Bonding* **2005**, *118*, 79–119.
- (12) (a) Battaglia, D.; Blackman, B.; Peng, X. *J. Am. Chem. Soc.* **2005**, *127*, 10889–10897. (b) Milliron, D. J.; Hughes, S. M.; Cui, Y.; Manna, L.; Li, J.; Wang, L.-W.; Alivisatos, A. P. *Nature (London)* **2004**, *430*, 190–195. (c) Erwin, S. C.; Zu, L.; Haftel, M. I.; Efros, A. L.; Kennedy, T. A.; Norris, D. J. *Nature (London)* **2005**, *436*, 91–94.
- (13) (a) Asokan, S.; Krueger, K. M.; Alkhawaldeh, A.; Carreon, A. R.; Mu, Z.; Colvin, V. L.; Mantzaris, N. V.; Wong, M. S. *Nanotechnology* **2005**, *16*, 2000–2011. (b) Deng, Z. T.; Cao, L.; Tang, F. Q.; Zou, B. S. *J. Phys. Chem. B* **2005**, *109*, 16671–16675.
- (14) (a) Sapra, S.; Rogach, A. L.; Feldmann, J. *J. Mater. Chem.* **2006**, *16*, 3391–3395. (b) Jasieniak, J.; Bullen, C.; van Embden, J.; Mulvaney, P. *J. Phys. Chem. B* **2005**, *109*, 20665–20668. (c) Yang, Y. A.; Wu, H.; Williams, K. R.; Cao, Y. C. *Angew. Chem., Int. Ed.* **2005**, *44*, 6712–6715.
- (15) (a) Qu, L.; Peng, X. *J. Am. Chem. Soc.* **2002**, *124*, 2049–2055. (b) Pradhan, N.; Reifsnnyder, D.; Xie, R. G.; Aldana, J.; Peng, X. *J. Am. Chem. Soc.* **2007**, *129*, 9500–9509. (c) Yen, B. K. H.; Gunther, A.; Schmidt, M. A.; Jensen, K. F.; Bawendi, M. G. *Angew. Chem., Int. Ed.* **2005**, *44*, 5447–5451.
- (16) (a) Steckel, J. S.; Yen, B. K. H.; Oertel, D. C.; Bawendi, M. G. *J. Am. Chem. Soc.* **2006**, *128*, 13032–13033. (b) Liu, H.; Owen, J. S.; Alivisatos, A. P. *J. Am. Chem. Soc.* **2007**, *129*, 305–312.
- (17) Pan, D. C.; Jiang, S. C.; An, L. J.; Jiang, B. Z. *Adv. Mater.* **2004**, *16*, 982–985.
- (18) Madelung, O., Ed. *Numerical Data and Functional Relationships in Science and Technology. Group III: Crystal and Solid State Physics*; Vol. 17b: Physics of II–VI and I–VII Compounds, Semi-Magnetic Semiconductors, Landolt-Börnstein Series; Springer: Berlin, Germany, 1982.
- (19) Embden, J. V.; Mulvaney, P. *Langmuir* **2005**, *21*, 10226–10233.
- (20) Talapin, D.; Rogach, A. L.; Kornowski, A.; Haase, M.; Weller, H. *Nano Lett.* **2001**, *1*, 207–211.
- (21) Hu, J.; Li, L. S.; Yang, W. D.; Manna, L.; Wang, L. W.; Alivisatos, A. P. *Science* **2001**, *292*, 2060–2063.
- (22) Ninomiya, S.; Adachi, S. *J. Appl. Phys.* **1995**, *78*, 4681–4689.
- (23) (a) Jasieniak, J.; Mulvaney, P. *J. Am. Chem. Soc.* **2007**, *129*, 2841–2848. (b) Munro, A. M.; Jen-Là Plante, I.; Ng, M. S.; Ginger, D. S. *J. Phys. Chem. C* **2007**, *111*, 6220–6227.
- (24) (a) Tang, Z.; Kotov, N. A.; Giersig, M. *Science* **2002**, *297*, 237–240. (b) Shim, M.; Guyot-Sionnest, P. *J. Chem. Phys.* **1999**, *111*, 6955–6964.
- (25) (a) Navrotsky, A. *Proc. Natl. Acad. Sci. U.S.A.* **2004**, *101*, 12096–12101. (b) Niederberger, M.; Cölfen, H. *Phys. Chem. Chem. Phys.* **2006**, *8*, 3271–3287.
- (26) Shevchenko, E. V.; Talapin, D. V.; Schnablegger, H.; Kornowski, A.; Festin, Ö.; Svedlindh, P.; Haase, M.; Weller, H. *J. Am. Chem. Soc.* **2003**, *125*, 9090–9101.
- (27) Mullin, J. W. *Crystallization*, 4th ed.; Butterworth-Heinemann: Boston, MA, 2001.
- (28) (a) Spanhel, L.; Anderson, M. A. *J. Am. Chem. Soc.* **1991**, *113*, 2826–2833. (b) Ptatscheck, V.; Schmidt, T.; Lerch, M.; Müller, G.; Spanhel, L.; Emmerling, A.; Fricke, J.; Foitzik, A. H.; Langer, E. *Ber. Bunsenges. Phys. Chem.* **1998**, *102*, 85–95. (c) Spanhel, L. *J. Sol-Gel Sci. Technol.* **2006**, *39*, 7–24. (d) Vossmeyer, T.; Reck, G.; Katsikas, L.; Haupt, E. T. K.; Schulz, B.; Weller, H. *Science* **1995**, *267*, 1476–1479. (e) Feng, P.; Bu, X.; Zheng, N. *Acc. Chem. Res.* **2005**, *38*, 293–303. (f) Zhang, T. H.; Liu, X. Y. *Angew. Chem., Int. Ed.* **2009**, *48*, 1–6.
- (29) (a) Wang, Y.; Herron, N. *J. Phys. Chem.* **1991**, *95*, 525–532. (b) Herron, N.; Suna, A.; Wang, Y. *J. Chem. Soc., Dalton Trans.* **1992**, 2329–2335. (c) Lee, G. S. H.; Craig, D. C.; Ma, I.; Scudder, M. L.; Bailey, T. D.; Dance, I. G. *J. Am. Chem. Soc.* **1988**, *110*, 4863–4864. (d) Corrigan, J. F.; Fuhr, O.; Fenske, D. *Adv. Mater.* **2009**, *21*, 1–5.
- (30) (a) Barglik-Chory, Ch.; Münster, A. F.; Strohm, H.; Remenyi, Ch.; Müller, G. *Chem. Phys. Lett.* **2003**, *374*, 319–325. (b) Dagtepe, P.; Chikan, V.; Jasinski, J.; Leppert, V. *J. J. Phys. Chem. C* **2007**, *111*, 14977–14983. (c) Dagtepe, P.; Chikan, V. *J. Phys. Chem. A* **2008**, *112*, 9304–9311. (d) Tuinenga, C.; Jasinski, J.; Iwamoto, T.; Chikan, V. *ACS Nano* **2008**, *2*, 1411–1421.
- (31) (a) Løver, T.; Bowmaker, G.; Seakins, J. M.; Cooney, R. P.; Henderson, W. *J. Mater. Chem.* **1997**, *7*, 647–651. (b) Løver, T.; Henderson, W.; Bowmaker, G.; Seakins, J. M.; Cooney, R. P. *Inorg. Chem.* **1997**, *36*, 3711–3723. (c) Cumberland, S. L.; Hanif, K. M.; Javier, A.; Khitrov, G. A.; Strouse, G. F.; Woessner, S. M.; Yun, C. S. *Chem. Mater.* **2002**, *14*, 1576–1584.
- (32) Trout, B. L.; Bawendi, M. G.; Jensen, K. F. *J. Phys. Chem. B* **2006**, *110*, 18007–18016.
- (33) Kuno, M.; Lee, J. K.; Dabbousi, B. O.; Mikulec, F. V.; Bawendi, M. G. *J. Chem. Phys.* **1997**, *106*, 9869–9882.
- (34) Zhong, X. H.; Feng, Y. Y.; Zhang, Y. L. *J. Phys. Chem. C* **2007**, *111*, 526–531.
- (35) Zhang, Z.; Zhong, X.; Liu, S.; Li, D.; Han, M. *Angew. Chem., Int. Ed.* **2005**, *44*, 3466–3470.
- (36) Guo, W.; Li, J. J.; Wang, Y. A.; Peng, X. *J. Am. Chem. Soc.* **2003**, *125*, 3901–3909.
- (37) (a) Dabbousi, B. O.; Rodriguez-Viejo, J.; Mikulec, F. V.; Heine, J. R.; Mattoussi, H.; Ober, R.; Jensen, K. F.; Bawendi, M. G. *J. Phys. Chem. B* **1997**, *101*, 9463–9475. (b) Peng, X.; Schlamp, M. C.; Kadavanich, A. V.; Alivisatos, A. P. *J. Am. Chem. Soc.* **1997**, *119*, 7019–7029.
- (38) (a) Tiemann, M.; Marlow, F.; Brieler, F.; Lindén, M. *J. Phys. Chem. B* **2006**, *110*, 23142–23147. (b) Abécassis, B.; Testard, F.; Spalla, O.; Barboux, P. *Nano Lett.* **2007**, *7*, 1723–1727.
- (39) (a) Pradhan, N.; Goorskey, D.; Thessing, J.; Peng, X. *J. Am. Chem. Soc.* **2005**, *127*, 17586–17587. (b) Mai, H. X.; Zhang, Y. W.; Sun, L. D.; Yan, C. H. *J. Phys. Chem. C* **2007**, *111*, 13721–13729.

JP811308H